Polymer Chemistry

RSC Publishing

PAPER

View Article Online
View Journal | View Issue

Cite this: *Polym. Chem.*, 2013, **4**, 1199

pH and reduction dual-responsive nanogel cross-linked by quaternization reaction for enhanced cellular internalization and intracellular drug delivery†

Mingqiang Li,[ab] Zhaohui Tang,[a] Hai Sun,[a] Jianxun Ding,[ab] Wantong Song[ab] and Xuesi Chen*[a]

A novel pH and reduction dual-responsive nanogel with improved cellular internalization was prepared through atom transfer radical polymerization and subsequent quaternization reaction. Doxorubicin (DOX), a model anticancer drug, was loaded into the nanogel *via* dispersion. The DOX-loaded nanogel presented a stable core-cross-linked structure under physiological conditions, but quickly released its payload in an acidic (pH 6.8) and reductive (10.0 mM glutathione) environment. Confocal fluorescence microscopy and fluorescence flow cytometry revealed that the DOX-loaded nanogel could deliver DOX into the cytoplasm and nucleus of cells, more efficiently than that of free DOX. The improved cellular internalization was more significant under acidic and reductive conditions, which was analogous to the pH and reductive conditions in endosomes and cytoplasm. *In vitro* cytotoxicity studies demonstrated that the pH and reduction responsive DOX-loaded nanogel could inhibit cellular proliferation more efficiently than free DOX. This dual-bioresponsive nanogel with quaternary ammonium salt group has appeared to be highly promising in the further development of intracellular drug transporters.

Received 18th October 2012
Accepted 6th November 2012

DOI: 10.1039/c2py20871g

www.rsc.org/polymers

Introduction

Nano-scaled amphiphilic polymeric nanocarriers have attracted much attention as potential drug carriers because of their distinct advantages, including versatile physicochemical properties, improved drug solubility, prolonged circulation time through avoiding rapid clearance by the renal and reticuloendothelial systems (RES), decreased side effects, passive targeting of tumor tissues *via* the enhanced permeability and retention (EPR) effect, and improved drug bioavailability.[1–3] Of these nanoparticles, the polymeric micelle is one of the most common and important species. However, the low *in vivo* structural stability of micelles often leads to micelle dissociation at concentrations below the critical micelle concentration (CMC), which will cause the loss of drug during blood circulation and limit their further clinical applications.[1,4] Many attempts have been made to improve the physical stability of polymeric micelles through various cross-linking approaches in the past several years. The cross-linking of micelles could take place in the hydrophilic shell,[5] the hydrophobic or ionizable core,[6,7] or the core–shell interface.[8]

Nevertheless, the loaded drug should be released specifically and rapidly at the site of action to maximize the therapeutic effect. The cross-linked carriers may indeed act as a barrier to intracellular drug release. Consequently, the introduction of biodegradable linkages for cross-linking is especially essential for drug release.[1] Up to now, many stimuli-responsive nanocarriers based on external triggers (such as ultrasound, magnetic field and light) and changes to the local microenvironment of the disease site (such as pH, temperature and redox-potential) have been rationally exploited to achieve controlled drug release at the targeted sites. Among current responsive drug-delivery systems, pH change and redox potential are major chemical stimuli to trigger drug release from cargos. Taking advantage of the differences in certain pathological sites and/or intracellular compartments, carriers formulated with pH and redox sensitivities are promising for biomedical applications.

In comparison to the physiological condition, solid tumors always present as acidic condition (tissue pH ~6.0 to 7.0) due to the Warburg effect,[9] which might be attributed to the inefficient consumption of glucose into energy in cancer cells producing a large amount of lactic acid.[10,11] The intracellular compartments are characterized by various pH values, while the pH is maintained at about 7.4 in normal extracellular matrices and blood. The drug delivery system is internalized by the cell through

[a]*Key Laboratory of Polymer Ecomaterials, Changchun Institute of Applied Chemistry, Chinese Academy of Sciences, Changchun 130022, P. R. China. E-mail: xschen@ciac.jl.cn; Fax: +86 431 85262112; Tel: +86 431 85262112*

[b]*Graduate University of the Chinese Academy of Sciences, Beijing 100039, P. R. China*

† Electronic supplementary information (ESI) available: The ^{1}H, ^{13}C NMR spectra and MALDI-TOF MS spectrum of *N*,*N*′-bis(bromoacetyl) cystamine. THF GPC traces recorded for mPEG-Br and mPEG-*b*-PDEA. Raman spectra of mPEG-*b*-PDEA and disulfide core-cross-linked mPEG-*b*-PDEA nanogel. Potentiometric titration curve obtained for the aqueous solution of core-cross-linked mPEG-*b*-PDEA nanogel. Hydrodynamic radius distributions of core-cross-linked nanogel in $CHCl_3$ and THF. See DOI: 10.1039/c2py20871g

endocytosis into a clathrin-coated vesicle that fuses to form an early endosome (pH ~6.0 to 7.4), then a late endosome (pH ~5.5 to 6.0), and eventually lysosomes (pH ~5.0).[12,13] Accordingly, many pH-responsive polymeric nanocarriers have been developed for tumor targeting and intracellular drug release.[14–16] The "titratable" groups, such as tertiary amines or carboxylic acids,[17,18] are often introduced into amphiphilic polymers, so that micelle formation or disintegration can be controlled by the protonation or deprotonation of these groups.[19]

It has been reported that reduced glutathione (GSH), a tripeptide containing cysteine, is found at different concentrations in the cytosol (~0.5 to 10.0 mM) and extracellular fluids (~2.0 to 20.0 μM), and even at higher levels in cancer cells.[20,21] As a reductively cleavable linkage, the disulfide bond is known to rupture rapidly in response to the intracellular reductive environment, due to the thiol–disulfide exchange reaction with small redox molecules (*e.g.* GSH).[22,23] Disulfide bonds, therefore, are stable under physiological conditions in the circulation as well as in extracellular tissues due to a low concentration of GSH, but will quickly degrade in a highly reductive environment in cells.[19] In recent years, reductively degradable nano-vehicles have emerged as unique intracellular delivery systems for various bioactive molecules including chemotherapeutics,[24] DNA,[25] siRNA,[26] antisense oligonucleotide (asODN)[22] and proteins.[27] With respect to the molecular level, the disulfide linkage is a typical characteristic of reduction-sensitive polymeric nanocarriers, and is usually located in the main chains,[28] side chains or cross-linkers.[29,30]

Very recently, several reports have appeared concerning pH and reduction dual-sensitive polymeric drug carriers. Zhong's group prepared pH and reduction dual-responsive nanosized polymersomes based on poly(ethylene glycol)–SS–poly(2-(diethylamino)ethyl methacrylate) (PEG–SS–PDEA) diblock copolymers for efficient encapsulation and triggered intracellular release of proteins.[27] Li and co-workers prepared pH and redox-responsive polysaccharide-based microcapsules through dynamic covalent assembly of a Schiff base and disulfide for docetaxel delivery.[31] Xing and co-workers designed and synthesized a novel copolymer based on poly(ethylene glycol) (PEG) and reducible poly(β-amino ester)s (RPAE), containing disulfide bonds in the backbone of poly(β-amino ester)s for intracellular DOX delivery.[19] Chen *et al.* developed two kinds of novel disulfide-cross-linked poly(ethylene glycol)-polypeptide copolymers with ionizable cores for efficient doxorubicin (DOX) loading and triggered release.[32]

In addition, quaternary ammonium salts have been shown to have excellent activity to penetrate the outer membranes of many cell types and to display high transfection activities in gene delivery. Thus, the quaternary ammonium salt-containing nanocarriers are used as drug and gene carriers.[33,34]

In this paper, we described a novel pH and reduction dual-sensitive drug delivery system cross-linked by a quaternary ammonium salt through a two-step approach. First, monomethoxyl poly(ethylene glycol)-*block*-poly-(*N*,*N*′-diethylaminoethyl methacrylate) (mPEG-*b*-PDEA) was prepared by atom transfer radical polymerization (ATRP), using a mPEG-based macroinitiator (mPEG-Br). Then, polymeric nanogels cross-linked by *N*,*N*′-bis(bromoacetyl) cystamine were fabricated *via* quaternization reaction between the nitrogen from DEA and the bromine from the cross-linker. The dual-bio-responsive nanogel functionalized with quaternary ammonium salt could efficiently accelerate cellular internalization. Also, it is likely destabilized in the acidic endo/lysosomal compartments by ionization of PDEA block as well as in the cytoplasm by cleavage of the intervening disulfide bonds, resulting in efficient intracellular release of anticancer drugs. The loading and *in vitro* release of DOX, and the cellular proliferation inhibition and cellular internalization behavior of DOX-loaded nanogel were investigated.

Experimental section

Materials

Pentamethyldiethylenetriamine (PMDETA, 99%), branched polyethylenimine (average M_w ~25 000, PEI25k), and mPEG (M_n = 5000) were purchased from Aldrich and used without further purification. 2-Bromoisobutyryl bromide (97%) and bromoacetyl bromide (98%) were purchased from Alfa Aesar and used as obtained. 2-(Diethylamino)ethyl methacrylate (DEA, 99%, Aldrich) was dried with calcium hydride, vacuum-distilled, and stored at −20 °C prior to use. GSH (used for cell culture) and D,L-1,4-dithiothreitol (DTT) were purchased from Aladdin Reagent Company (Shanghai). Cystamine dihydrochloride and doxorubicin hydrochloride (DOX·HCl) were purchased from Shanghai Darui Finechemical Co., Ltd. and Beijing Huafeng United Technology Corporation, respectively. 3-(4,5-Dimethyl-thiazol-2-yl)-2,5-diphenyl tetrazolium bromide (MTT) and 4′,6-diamidino-2-phenylindole dihydrochloride (DAPI) were purchased from Sigma and used as received. Clear polystyrene tissue culture treated 6-well and 96-well plates were obtained from Corning Costar. Purified deionized water was prepared by the Milli-Q plus system (Millipore Co., Billerica, MA, USA).

Measurements

^{1}H and ^{13}C NMR spectra were recorded on a Bruker AV 300 NMR spectrometer in chloroform ($CDCl_3$). Raman spectroscopy was measured using a FT-Raman spectrometer (Thermo Nicolet 960) equipped with an InGaAs detector and Nd/VO4 laser (1064 nm) as an excitation source. Gel-permeation chromatography (GPC) analysis was conducted on a Waters 2414 system equipped with Waters HT4 and HT3 column-assembly and a Waters 2414 refractive index detector (eluent: tetrahydrofuran (THF); flow rate: 1.0 mL min^{-1}; temperature: 40 °C; standard: polystyrene). Dynamic laser scattering (DLS) measurements were performed on a WyattQELS instrument with a vertically polarized He–Ne laser (DAWN EOS, Wyatt Technology). The scattering angle was fixed at 90°. Transmission electron microscopy (TEM) measurements were performed on a JEOL JEM-1011 transmission electron microscope with an accelerating voltage of 100 KV. The MALDI-TOF MS experiment was performed on an Autoflex III TOF/TOF Analyzer (Bruker Daltonics Inc., Germany).

Synthesis of mPEG-Br macroinitiator

The macroinitiator, mPEG-Br was prepared following a previously published protocol with minor modification.[35] Briefly, to a dry 250 mL round bottom flask equipped with a magnetic stirrer, mPEG (20.0 g, 4.0 mmol) was added, and the flask was placed in an oil bath at 120 °C under vacuum, and maintained at this temperature for 5 h. After cooling to room temperature, dichloromethane (200.0 mL) and triethylamine (TEA or Et_3N, 1.2 g, 12.0 mmol) were added. When the mixture was cooled to 0 °C, 2-bromoisobutyryl bromide (5.5 g, 24.0 mmol) was added dropwise over 30 min. Then the reaction mixture was stirred at room temperature for 24 h. The $Et_3N \cdot HBr$ salt was removed by filtering and then the solution was concentrated, followed by precipitation in cold diethyl ether to obtain the crude product. The residue was dissolved in dichloromethane (150.0 mL) and washed with a saturated aqueous solution of $NaHCO_3$ (20.0 mL × 3) and 5.0 wt% NaCl (20.0 mL). The organic layer was separated and dried over anhydrous $MgSO_4$ overnight, filtered and concentrated in vacuum. The purified macroinitiator was isolated by precipitation in cold diethyl ether and dried *in vacuo* (yield: 85.3%).

Synthesis of mPEG-*b*-PDEA diblock copolymer

mPEG-*b*-PDEA diblock copolymer was prepared by the ATRP of DEA monomer using mPEG-Br and CuBr/PMDETA as macroinitiator and catalyst, respectively. A reaction flask equipped with a magnetic stirring bar and a rubber septum was charged with mPEG-Br macroinitiator (3.6 g, 0.7 mmol), DEA (7.8 g, 42.0 mmol), PMDETA (123.1 mg, 0.7 mmol) and isopropanol (IPA, 12.0 mL). The flask was degassed by three freeze–pump–thaw cycles and backfilled with argon. CuBr (100.4 mg, 0.7 mmol) was added to start the polymerization under the protection of Ar flow. The flask was then sealed under vacuum and placed in an oil bath thermostatted at 50 °C. The reaction solution turned dark green and more viscous as the polymerization proceeded. After 6 h, the reaction mixture was exposed to air and diluted with 15.0 mL THF. The mixture was then passed through a silica gel column to remove copper catalyst. After removing all the solvents by a rotary evaporator, the residues were dissolved in CH_2Cl_2 and purified by repeated precipitation into *n*-hexane to remove unreacted monomer. The final product was dried in a vacuum oven overnight at room temperature, yielding a white solid (8.7 g, yield: 76.8%).

Synthesis of *N*,*N*′-bis(bromoacetyl) cystamine

N,*N*′-Bis(bromoacetyl) cystamine (BBAC) was synthesized using similar procedures to those described earlier.[36] Briefly, cystamine dihydrochloride (6.0 g, 26.6 mmol) was added into 75.0 mL of aqueous NaOH (4.26 g, 106.6 mmol) solution in a 150.0 mL round-bottom flask. A solution of bromoacetyl bromide (10.76 g, 53.3 mmol) in 10.0 mL dichloromethane was added dropwise while stirring at 0 °C. After the addition was complete, the mixture was stirred at room temperature for 6 h. The solid product was obtained by filtration and dissolved in dichloromethane. The liquid phase was extracted with dichloromethane (20.0 mL × 3). The combined organic layers were dried over anhydrous Na_2SO_4 overnight. A white solid product was obtained after removing the solvent under reduced pressure (7.8 g, yield: 74%). The ^1H, ^{13}C NMR and MALDI-TOF MS spectra for BBAC are shown in Fig. S1–S3, respectively (ESI†).

Synthesis of core-cross-linked mPEG-*b*-PDEA nanogel

mPEG-*b*-PDEA diblock copolymer (0.2 g, 0.013 mmol) was dissolved in 100 mL acetonitrile (2 mg mL^{-1}) and heated to 50 °C. 14.3 mg *N*,*N*′-bis(bromoacetyl) cystamine (with the molar ratio of BBAC to DEA at 1/10) was then added to selectively cross-link the DEA residues. After stirring for 24 h, the solution was concentrated by rotary evaporation. The product was purified by dialysis (MWCO 3500 Da) against deionized water for 3 days and dried by lyophilization to give a white powder.

Potentiometric titration

The pK_a value of the nanogel was measured by acid–base titration method. The polymeric lyophilized powder was dissolved in deionized water (1.0 mg mL^{-1}) and adjusted to pH 3.0 with 0.1 M HCl. The solution was titrated by the dropwise addition of NaOH aqueous solution (0.01 M), and the pH was recorded to obtain a titration profile. The pK_a value of the nanogel was calculated from the derivative value of the titration curve, which corresponds to the inflection point.

Preparation of DOX-loaded nanogel

$DOX \cdot HCl$ (4.0 mg) and the lyophilized powder of the nanogel (40 mg) were dissolved in 10.0 mL deionized water (pH was adjusted to 6.0 with 0.01 M HCl) and stirred for 2 h. Then the pH was adjusted to 7.4 with a few drops of 0.01 M NaOH. The solution mixture was vigorously stirred overnight in the dark. Excess drug was removed by dialysis (MWCO 3500 Da) against deionized water for 24 h. The DOX-loaded nanogel was obtained by lyophilization in the dark.

For determination of drug loading content (DLC) and drug loading efficiency (DLE), lyophilized drug-loaded nanogel was dissolved in dimethylformamide and analyzed by fluorescence (Perkin-Elmer LS50B luminescence spectrometer) measurements using a standard curve method ($\lambda_{ex} = 480$ nm). The DLC and DLE were calculated according to the following formulae:

$$\text{DLC (wt\%)} = (\text{weight of loaded drug/weight of drug-loaded nanogel}) \times 100\%$$

$$\text{DLE (wt\%)} = (\text{weight of loaded drug/weight of feeding drug}) \times 100\%$$

In vitro DOX release

To determine the drug release of DOX from the DOX-loaded nanogel, the freeze-dried nanogel was suspended in phosphate buffered saline (PBS) at 0.2 mg mL^{-1} in the dialysis bag (MWCO 3500 Da), and immersed in 45.0 mL PBS (pH 6.8 or 7.4, with or without 10.0 mM GSH) at 37 °C with constant shaking. At

selected time intervals, 3.0 mL of solution outside the dialysis bag was removed for fluorescence analysis and replaced with the same volume of fresh PBS. The concentrations of DOX present in the dialysate were determined using fluorescence spectroscopy. The release experiments were conducted in triplicate and the presented results are the average data.

Cell culture

The human lung carcinoma (A549) cells were cultured at 37 °C in a 5% CO_2 atmosphere in Dulbecco's modified Eagle's medium (DMEM, Gibco) supplemented with 10% fetal bovine serum, penicillin (50 U mL^{-1}) and streptomycin (50 U mL^{-1}).

Confocal laser scanning microscopy (CLSM) observation

The cellular uptake and intracellular release behaviors of DOX-loaded nanogels were determined by CLSM towards A549 cells. The cells were seeded on the coverslips in 6-well plates at a density of 2×10^5 cells per well in 2.0 mL DMEM and cultured for 24 h, and then treated with GSH (used for cell culture) for 2 h. Cells were washed by PBS and the original medium was replaced with DOX-loaded nanogel (at a final DOX concentration of 5.0 mg L^{-1}) containing DMEM at pH 7.4 or 6.8. Cells without GSH treatment were used as the control. After 1 h incubation, the cells were washed and fixed with 4% formaldehyde for 20 min at room temperature, and the cell nuclei were stained with DAPI (blue). CLSM images of cells were obtained by a confocal microscope (Olympus FluoView 1000).

Cellular uptake measured by flow cytometry

A549 cells were seeded in 6-well plates with a density of 2×10^5 cells per well in 2.0 mL DMEM and incubated for 24 h, and then treated with GSH (used for cell culture) for 2 h. Cells were washed by PBS and the original medium was replaced with DOX-loaded nanogel (at a final DOX concentration of 5 mg L^{-1}) containing DMEM at pH 7.4 or 6.8. Cells without GSH treatment were used as the control. The cells were incubated for 1 h at 37 °C, and then washed thrice with PBS. The harvested cells were suspended in PBS and centrifuged at 1000 rpm for 5 min at 4 °C. The supernatants were discarded and the cells were washed with PBS to remove the background fluorescence in the media. After two cycles of washing and centrifugation, cells were resuspended with 500.0 μL PBS, and flow cytometry was done using a BD FACS Calibur flow cytometer from BD Biosciences.

Cytotoxicity assay

The cytotoxicities of nanogel and DOX-loaded nanogel against A549 cells were evaluated by a MTT assay. A549 cells were seeded in 96-well plates (1×10^4 cells per well) in 100 μL DMEM medium and incubated at 37 °C in a 5% CO_2 atmosphere for 24 h. The cells were then treated with GSH for 2 h. After washing off the GSH, the culture medium was replaced with 200 μL of fresh medium containing nanogel, free DOX or DOX-loaded nanogel. The cells were subjected to MTT assay after being incubated for another 24 h. The absorbance of the solution was measured on a Bio-Rad 680 microplate reader at 490 nm. The relative cell viability was determined by comparing the absorbance at 490 nm with control wells containing only cell culture medium. Data are presented as means ± SD ($n = 6$).

Results and discussion

Synthesis and characterization of core-cross-linked nanogel

pH and reduction-sensitive mPEG-*b*-PDEA nanogel with accelerated cellular internalization function was prepared *via* a two-step method (Scheme 1). Firstly, mPEG-*b*-PDEA copolymer was synthesized by ATRP using CuBr/PMDETA catalyst and mPEG-Br as the macroinitiator. The ^{1}H NMR spectrum of mPEG-*b*-PDEA copolymer recorded in $CDCl_3$ is displayed in Fig. 1A with the relevant signals labeled.

The actual degree of polymerization (DP) of PDEA block was determined to be 56 by comparing integration areas of peak b in the range of 3.70–3.50 ppm with that of peak f in the range of 4.20–3.98 ppm. The GPC trace (Fig. S4, ESI†) was mono-modal and quite symmetric, revealing a number average molecule weight (M_n) of 15 900 g mol^{-1} and polydispersity index (PDI, M_w/M_n) of 1.22. In comparison with that of mPEG-Br, the GPC trace of mPEG-*b*-PDEA exhibited a clear shift to the higher M_n region, indicating an almost quantitative initiating efficiency. ^{1}H NMR (Fig. 1A) and GPC analyses confirmed the successful synthesis of mPEG-*b*-PDEA with high purity and narrow polydispersity.

The pH and reduction dual-responsive polymeric nanogel was fabricated *via* selective cross-linking of the DEA residues by a bifunctional quaternizing agent (BBAC), accompanied by the formation of quaternary ammonium salt groups. This cross-linking reaction was carried out at 50 °C in acetonitrile for 24 h. On cooling to room temperature, the product was concentrated, purified by dialysis to remove the unreacted cross-linker and dried by lyophilization to give a white powder. Raman spectral measurements demonstrate the existence of the disulfide linkage (508 cm^{-1}, Fig. S5, ESI†).

Fig. 1B shows the ^{1}H NMR spectrum of the obtained polymeric nanogel. The signals corresponding to the mPEG arm (3.51 and 3.24 ppm) could be clearly seen, while the signals from the protons of the PDEA core were significantly suppressed in the ^{1}H NMR spectrum. The results were believed to be attributed to the reduced mobility of the cross-linked segment of the inner core.[37,38] Then a reductive condition mimicking the intracellular circumstance was employed to check whether the nanogel could be de-cross-linked. The ^{1}H NMR spectrum was measured after disassembly by adding DTT, a reducing agent for breaking disulfide linkages. As shown in Fig. 1C, the disassembly of the core-cross-linked nanogel occurred after adding DTT, which led to the liberation of free linear polymer chains. Nearly all the characteristic peaks corresponding to the PDEA segment were observed after reduction with DTT. For example, chemical shifts at 0.88 and 1.05 ppm were attributed to the protons of methyl groups (c and g) of the PDEA block. The appearance of these characteristic peaks after reduction were attributed to the decrease of the cross-linking density due to the cleavage of disulfide bonds, and further confirmed that

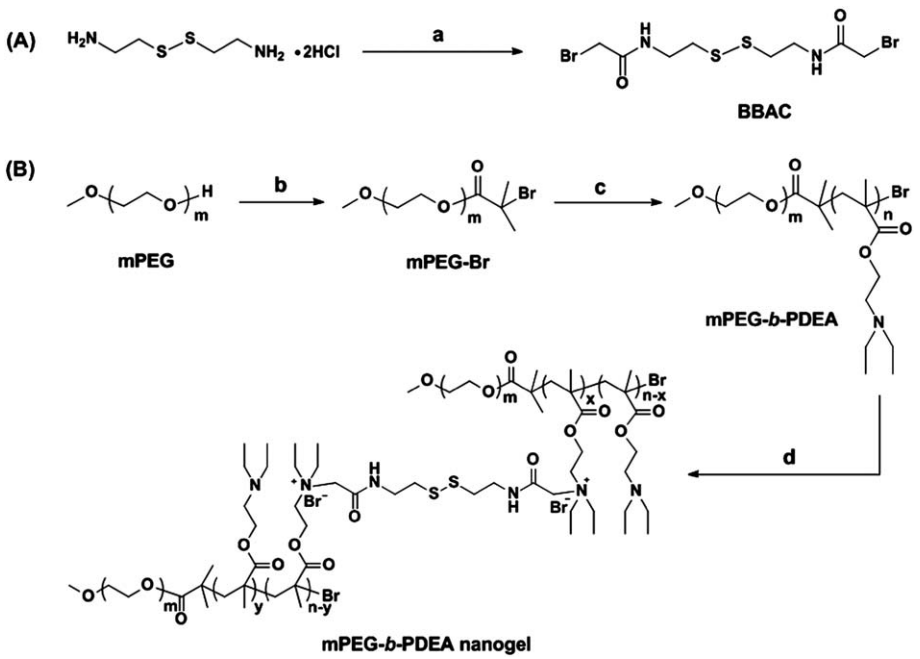

Scheme 1 Synthesis of disulfide core-cross-linked nanogel. *Reagents and conditions*: (a) bromoacetyl bromide, NaOH, CH_2Cl_2, 0 °C for 0.5 h, room temperature for 24 h; (b) 2-bromoisobutyryl bromide, TEA, CH_2Cl_2, 0 °C to room temperature, 6 h; (c) DEA, CuBr, PMDETA, IPA, 50 °C, 6 h; and (d) acetonitrile, BBAC, 50 °C, 24 h.

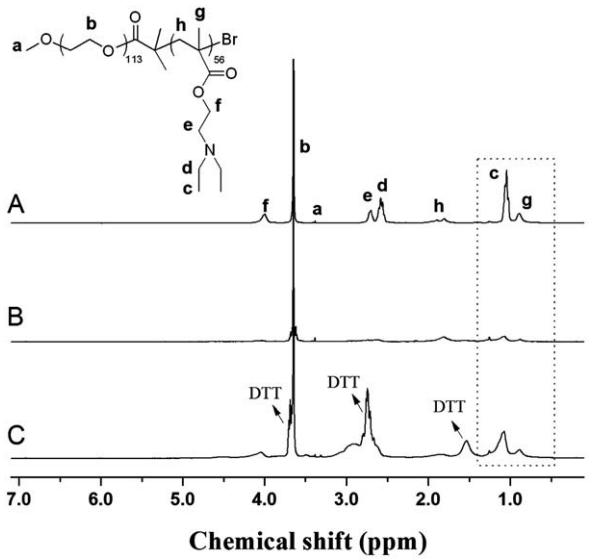

Fig. 1 ^{1}H NMR spectra obtained in $CDCl_3$ for (A) mPEG-*b*-PDEA, (B) core-cross-linked mPEG-*b*-PDEA nanogel and (C) nanogel after reduction with DTT.

the mobility of the polymer was significantly restricted by the cross-linked core.[38]

PDEA homopolymer is a weak polybase and its conjugated acid possesses a pK_a of ~7.3.[39] It is water-insoluble at neutral or alkaline pH. Whereas below pH 6.0, it is soluble as a weak cationic polyelectrolyte due to protonation of tertiary amine residues.[40] The potentiometric titration result in aqueous solution indicated that the core-cross-linked nanogel buffered the solution in the pH range of 6.0–8.0, and the pK_a was determined to be 7.0, which was slightly lower than that of PDEA homopolymer (Fig. S6, ESI†). This might be due to the high local chain density of PDEA sequences within the core-cross-linked nanogel.[41]

The TEM micrograph showed that the core-cross-linked nanogel took a clear spherical morphology with a respective average radius of around 50 nm (Fig. 2A). In contrast, the hydrodynamic radius (R_h) measured by DLS was 60 ± 9 nm. The smaller size from TEM observations should be due to the dehydration of the nanogel in the TEM sample preparation process.[6]

Due to the presence of PEG shells, the nanogel can be well distributed in aqueous and organic solutions including $CHCl_3$, THF, dimethyl sulfoxide (DMSO), and 1,4-dioxane. When the nanogel was distributed in $CHCl_3$ and THF, it swelled and the average R_h values were 98 ± 15 and 90 ± 12 nm, respectively (Fig. S7, ESI†), indicating the successful formation of core-cross-linked nanogels.[42] For comparison, no laser scattering signals for the particle size of the solutions of mPEG-*b*-PDEA were determined (data not shown). The larger hydrodynamic radii of the core-cross-linked mPEG-*b*-PDEA nanogels in $CHCl_3$ and THF as compared with that measured in water (60 ± 9 nm), could be explained by the swelling propensity of the core-cross-linked nanogel in good organic solvents.[42–44]

From the combined results of ^{1}H NMR, TEM, potentiometric titration and DLS measurements, it can be concluded that the as-prepared polymeric nanogel has a pH responsive PEGylated disulfide core-cross-linked structure.

Drug loading and triggered release

DOX, an anthracycline anticancer drug, is widely used to treat different types of solid malignant tumors, *via* insertion of DNA

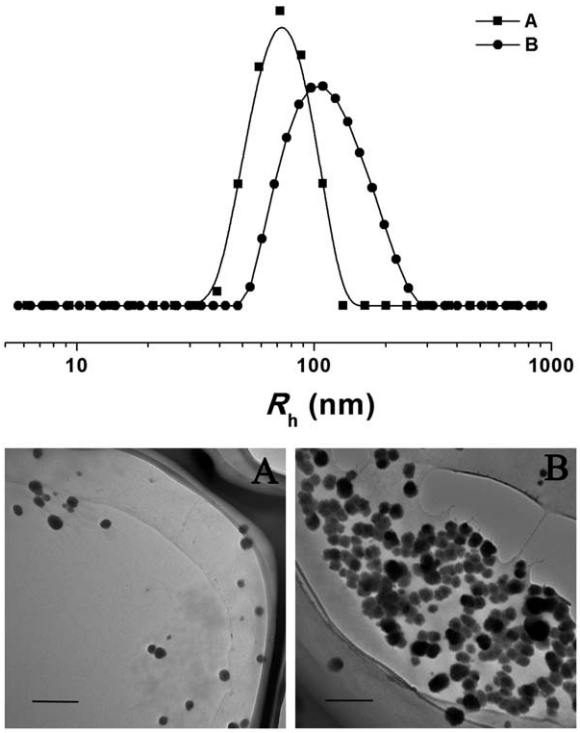

Fig. 2 Hydrodynamic radius distributions and morphologies of (A) core-cross-linked mPEG-*b*-PDEA nanogel and (B) DOX-loaded nanogel (scale bars: 500 nm).

or RNA to inhibit the biosynthesis of bioactive macromolecules.[6,45] In this study, core-cross-linked mPEG-*b*-PDEA nanogel was designed for active loading and triggered intracellular delivery of DOX (Scheme 2). DOX-loaded nanogel was readily prepared by adjusting the pH of mPEG-*b*-PDEA nanogel and DOX aqueous solution to 6.0 and stirring for 30 min. The pH of the solution was adjusted to 7.4 with a few drops of 0.01 M NaOH, and then the free DOX was removed by extensive dialysis. The increase of pH would lead to shrinking of the nanogel core and wrapping of the drug molecule in the hydrophobic core. The DLC and DLE were calculated to be 6.6 and 70.7 wt%, respectively. The particle size of DOX-loaded nanogel increased in comparison to the pure nanogel (Fig. 2B), which can be attributed to the interaction between the hydrophobic DOX and hydrophobic PDEA core of the micelle.[46]

The DOX release behaviors of the nanogel were investigated with and without GSH at pH 6.8 and 7.4 using the dialysis method. The cumulative release percentages of DOX loaded in the nanogel *versus* time are plotted in Fig. 3. In the absence of 10.0 mM GSH, minimal (less than 25%) loaded DOX was released from the nanogel in 72 h at pH 7.4. This result indicated that the DOX-loaded nanogel would preserve its core-cross-linked structure at physiological pH, resulting in a slow release. When the drug-loaded nanogel was dispersed in an acidic environment with pH lower than 6.8, the drug entrapped in the core would quickly release with the expansion of the core-cross-linked nanogel, which resulted from the protonation of PDEA and the electrostatic repulsion. As shown in Fig. 3B, the release of DOX was significantly accelerated at pH 6.8 due to protonation of PDEA, for which 62% of DOX was released in 72 h. The great difference in GSH levels between blood circulation (~10.0 to 100.0 μM) and tumor cell (~1 to 10.0 mM) may trigger cleavage of the disulfide bonds and disassemble the core-cross-linked nanogel, which results in a burst-release of the incorporated drug from the nanogel in the tumor cell. As expected, the solution at pH 7.4 or 6.8 with 10.0 mM GSH led to a rapid reductive degradation of the PDEA core followed by a triggered fast release of the loaded DOX. The rate of DOX released from the nanogel at pH 6.8 and 10.0 mM GSH was clearly faster than that at pH 6.8 without GSH or pH 7.4 with 10 mM GSH. As shown in Fig. 3A, over 90% of loaded DOX was released at pH 6.8 with 10.0 mM GSH in 72 h. Therefore, the acidic and reductive condition accelerated drug release indicated that the DOX-loaded nanogel would be suitable for intracellular drug delivery.

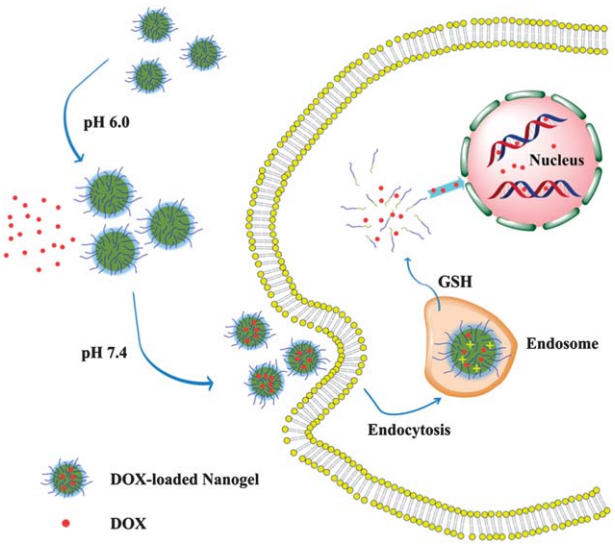

Scheme 2 Schematic illustration of drug loading, endocytosis and intracellular drug release of the pH and reduction dual-responsive nanogel.

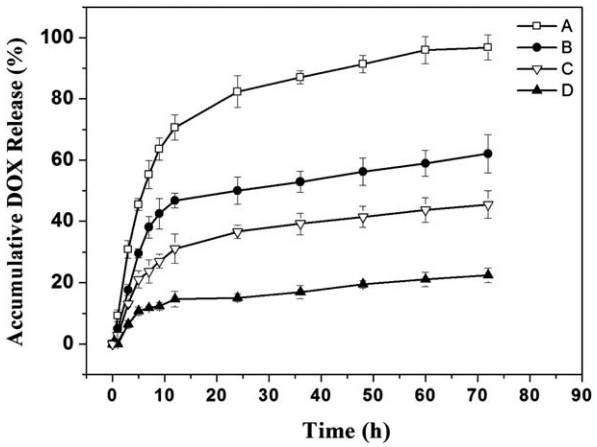

Fig. 3 pH and/or reduction-triggered DOX release from DOX-loaded nanogel in PBS: (A) pH 6.8 with 10.0 mM GSH, (B) pH 6.8, (C) pH 7.4 with 10.0 mM GSH and (D) pH 7.4.

Intracellular DOX release

To investigate the cellular internalization and the pH and reduction dual-sensitive intracellular release of DOX, the DOX-loaded nanogel was incubated with A549 cells for 1 h at 37 °C. The cells in the culture media were pretreated with 10.0 mM GSH for 2 h. The cells were then observed by CLSM. The nuclei of A549 cells were selectively stained with DAPI to visualize the nuclear region. Red fluorescence imaging was performed to visualize the released DOX (Fig. 4). As expected, stronger red fluorescence in cells was clearly observed. As shown in Fig. 4, the fluorescence intensity decreased in the following order: DOX loaded nanogel at pH 6.8 in GSH pretreated cells > DOX loaded nanogel at pH 6.8 in GSH non-pretreated cells > DOX loaded nanogel at pH 7.4 in GSH pretreated cells > DOX loaded nanogel at pH 7.4 in GSH non-pretreated cells > free DOX at pH 7.4. For further confirmation, cellular internalization of DOX and DOX-loaded nanogel into the A549 cells were analyzed using fluorescence-activated flow cytometry (Fig. 5), and consistent results were acquired.

Several reports have demonstrated that the DOX molecule is membrane-permeable and can be internalized into tumor cells through a passive diffusion mechanism, while the DOX-loaded nanogel most likely needs to be endocytosed.[28,47,48] However, the quaternary ammonium functionalized nanogel and its capacity of penetrating the cytomembrane may increase the uptake of the nanogel.[33,49,50] As the CLSM results show in Fig. 4, the red fluorescence was mainly localized in the nucleus and near the cell membrane region for free DOX. In the case of the DOX-loaded nanogel at pH 7.4 without GSH pretreatment, the red fluorescence spread all over the cytoplasm and was accumulated in the nucleus. The fluorescence intensity of A549 cells cultured with the DOX-loaded nanogel was greatly enhanced under acidic conditions, and the cells pretreated with GSH showed a stronger fluorescence relative to those of non-pretreated. The enhancement of fluorescence signals in the acidic and reductive intracellular environments indicated the efficient cellular internalization, and rapid intracellular DOX release and

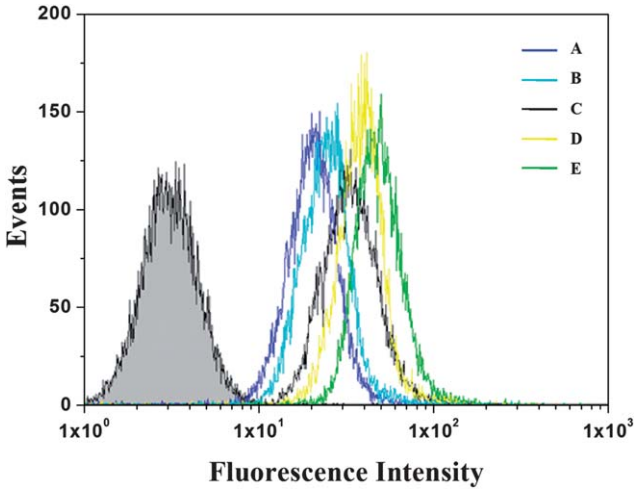

Fig. 5 The fluorescence activated cell sorting (FACS) analyses of cellular uptake of free DOX and DOX-loaded nanogel: (A) free DOX, pH 7.4; (B) DOX-loaded nanogel, pH 7.4; (C) DOX-loaded nanogel, pH 7.4, 10.0 mM GSH pretreated; (D) DOX-loaded nanogel, pH 6.8; and (E) DOX-loaded nanogel, pH 6.8, 10.0 mM GSH pretreated.

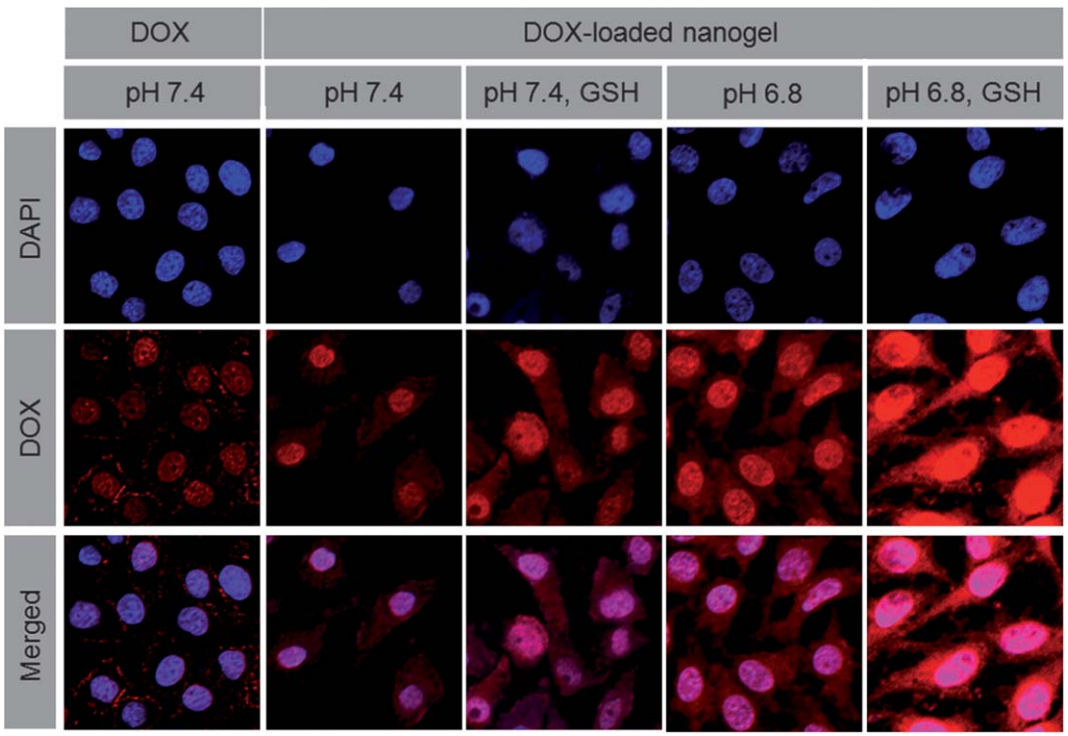

Fig. 4 Cellular uptake of DOX-loaded nanogel at pH 7.4, 6.8, and 7.4 and 6.8 in 10.0 mM GSH pretreated cells after incubation for 1 h.

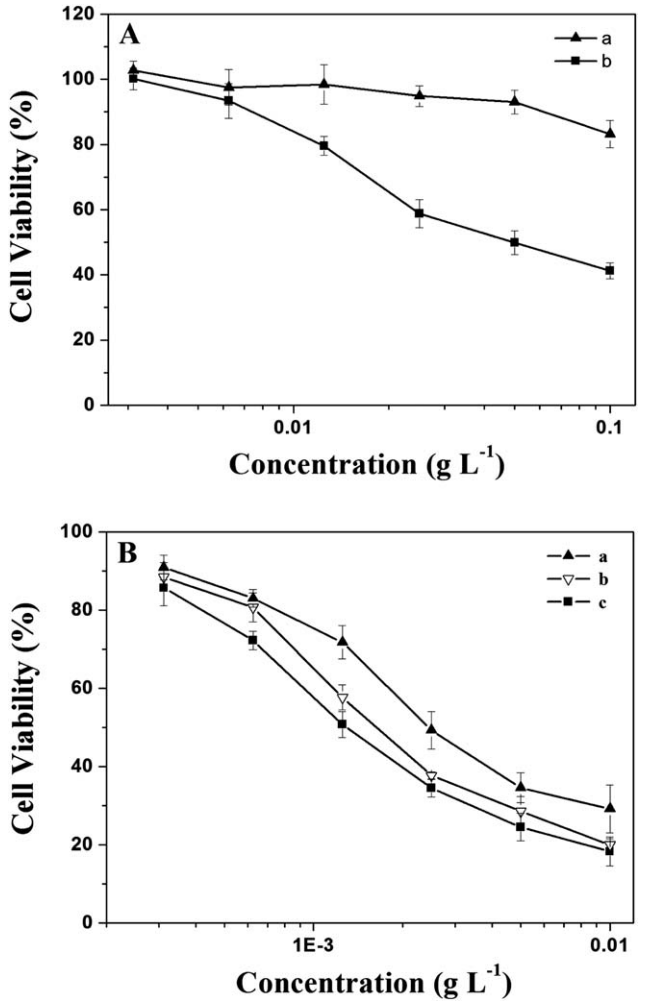

Fig. 6 (A) *In vitro* cytotoxicities of (a) core-cross-linked nanogel to A549 cells with (b) PEI25k as positive control; (B) the cytotoxicities of (a) free DOX, (b) non-pretreated and (c) 10.0 mM GSH pretreated A549 cells after 24 h incubation with DOX-loaded nanogel.

diffusion into nuclei of A549 cells, which could be easily explained by the cationic and disulfide cross-linked characteristics of the mPEG-*b*-PDEA nanogel.

Considering that the pH of the tissue and blood stream is about 7.4 (slightly higher than the pK_a of the nanogel), the nanogel cross-linked by disulfide bonds can protect the loaded DOX molecule. The extracellular pH of a tumor tissue is acidic (around pH 6.8),[51] which will result in the protonation of PDEA and the increased cellular internalization. The internalized nanogel could be rapidly disassembled and subsequently releases the drug at a high GSH level (approximately 0.5–10.0 mM) in the cytosol, which is about 2 to 3 orders higher than in the blood and extracellular fluids. Moreover, fluorescence analysis of tumor cells revealed that the DOX-loaded nanogel showed an increased fluorescence intensity at acidic pH, while pure DOX showed contrary results,[51] indicating that the DOX-loaded nanogel has tumor-extracellular pH-sensitive targetability. The above studies justify the uses of the nanogel for cytoplasmic drug delivery.

Cellular proliferation assay *in vitro*

The biocompatibility of the blank nanogel was estimated using a MTT assay toward A549 cells. The effect of nanogel concentration on the proliferation of the cells is shown in Fig. 6A. The results display that the copolymer did not exhibit apparent inhibition effects on cell proliferation at all the concentrations up to 0.1 g L^{-1}, indicating the good cytocompatibility of the nanogel.

The cytotoxicities of free DOX and DOX-loaded nanogel to A549 cells are compared in Fig. 6B. The cytotoxicity of DOX increased with the dose increase. A similar trend was observed for the DOX-loaded nanogels, which exhibited slightly higher cell inhibition efficiencies than free-DOX. Cells pretreated with GSH exhibited even higher inhibition efficacy. The possible reason was that the quaternary ammonium salt functionalized DOX-loaded nanogel had an excellent cell penetrating property for improved cellular internalization,[50] and rapidly released DOX triggered by both higher intracellular GSH concentration and lower endosomal pH.

Conclusions

A novel pH and reduction dual-responsive mPEG-*b*-PDEA nanogel was fabricated *via* quaternization of the nitrogen from DEA and bromine from *N*,*N*′-bis(bromoacetyl) cystamine. DOX was loaded into the nanogel, and the release behaviors of DOX from DOX-loaded nanogel could be regulated by pH and GSH concentration. A faster intracellular release of DOX from the nanogel occurred in GSH pretreated A549 cells at pH 6.8 than those of non-pretreated cells at pH 6.8 or 7.4. The cleavage of disulfide bonds triggered by intracellular GSH could accelerate the intracellular DOX release and thus enhance the *in vitro* cell proliferation inhibition. With convenient fabrication, good stability in the circulation condition and excellent drug loading and controlled release properties, the pH and reduction dual-responsive nanogel holds great potential for efficient intracellular delivery of potent anticancer drugs affording enhanced chemotherapy efficacy.

Acknowledgements

This research was financially supported by National Natural Science Foundation of China (Projects 20904053, 51173184, 21104076, 51233004 and 51021003), Ministry of Science and Technology of China (International Cooperation and Communication Program 2010DFB50890, 2011DFR51090), and Knowledge Innovation Program of the Chinese Academy of Sciences (Grant no. KJCX2-YW-H19).

Notes and references

1 Y. C. Wang, Y. Li, T. M. Sun, M. H. Xiong, J. Wu, Y. Y. Yang and J. Wang, *Macromol. Rapid Commun.*, 2010, **31**, 1201–1206.
2 H. F. Xu, F. H. Meng and Z. Y. Zhong, *J. Mater. Chem.*, 2009, **19**, 4183–4190.

3 J. Lu, S. C. Owen and M. S. Shoichet, *Macromolecules*, 2011, **44**, 6002–6008.
4 J. H. Na, H. Koo, S. Lee, K. H. Min, K. Park, H. Yoo, S. H. Lee, J. H. Park, I. C. Kwon, S. Y. Jeong and K. Kim, *Biomaterials*, 2011, **32**, 5252–5261.
5 L. Y. Lin, N. S. Lee, J. Zhu, A. M. Nyström, D. J. Pochan, R. B. Dorshow and K. L. Wooley, *J. Controlled Release*, 2011, **152**, 37–48.
6 J. X. Ding, F. H. Shi, C. S. Xiao, L. Lin, L. Chen, C. L. He, X. L. Zhuang and X. S. Chen, *Polym. Chem.*, 2011, **2**, 2857–2864.
7 Y. Vachutinsky, M. Oba, K. Miyata, S. Hiki, M. R. Kano, N. Nishiyama, H. Koyama, K. Miyazono and K. Kataoka, *J. Controlled Release*, 2011, **149**, 51–57.
8 K. Wang, G. F. Luo, Y. Liu, C. Li, S. X. Cheng, R. X. Zhuo and X. Z. Zhang, *Polym. Chem.*, 2012, **3**, 1084–1090.
9 L. Milane, S. Ganesh, S. Shah, Z.-f. Duan and M. Amiji, *J. Controlled Release*, 2011, **155**, 237–247.
10 M. G. V. Heiden, L. C. Cantley and C. B. Thompson, *Science*, 2009, **324**, 1029–1033.
11 H. J. Lee and Y. Bae, *Biomacromolecules*, 2011, **12**, 2686–2696.
12 Z. X. Zhou, Y. Q. Shen, J. B. Tang, M. H. Fan, E. A. Van Kirk, W. J. Murdoch and M. Radosz, *Adv. Funct. Mater.*, 2009, **19**, 3580–3589.
13 T. Liu, X. J. Li, Y. F. Qian, X. L. Hu and S. Y. Liu, *Biomaterials*, 2012, **33**, 2521–2531.
14 J. Ko, K. Park, Y. S. Kim, M. S. Kim, J. K. Han, K. Kim, R. W. Park, I. S. Kim, H. K. Song, D. S. Lee and I. C. Kwon, *J. Controlled Release*, 2007, **123**, 109–115.
15 A. Popat, J. Liu, G. Q. Lu and S. Z. Qiao, *J. Mater. Chem.*, 2012, **22**, 11173–11178.
16 K. E. Broaders, S. J. Pastine, S. Grandhe and J. M. J. Frechet, *Chem. Commun.*, 2011, **47**, 665–667.
17 P. S. Xu, E. A. Van Kirk, W. J. Murdoch, Y. H. Zhan, D. D. Isaak, M. Radosz and Y. Q. Shen, *Biomacromolecules*, 2006, **7**, 829–835.
18 E. F. Crownover, A. J. Convertine and P. S. Stayton, *Polym. Chem.*, 2011, **2**, 1499–1504.
19 J. Chen, X. Z. Qiu, J. Ouyang, J. M. Kong, W. Zhong and M. M. Q. Xing, *Biomacromolecules*, 2011, **12**, 3601–3611.
20 M. Ou, R. Z. Xu, S. H. Kim, D. A. Bull and S. W. Kim, *Biomaterials*, 2009, **30**, 5804–5814.
21 G. Saito, J. A. Swanson and K. D. Lee, *Adv. Drug Delivery Rev.*, 2003, **55**, 199–215.
22 F. H. Meng, W. E. Hennink and Z. Zhong, *Biomaterials*, 2009, **30**, 2180–2198.
23 H. Y. Wen, H. Q. Dong, W. J. Xie, Y. Y. Li, K. Wang, G. M. Pauletti and D. L. Shi, *Chem. Commun.*, 2011, **47**, 3550–3552.
24 Y. L. Li, L. Zhu, Z. Liu, R. Cheng, F. Meng, J. H. Cui, S. J. Ji and Z. Zhong, *Angew. Chem., Int. Ed.*, 2009, **48**, 9914–9918.
25 G. Y. Zhang, J. Liu, Q. Z. Yang, R. X. Zhuo and X. L. Jiang, *Bioconjugate Chem.*, 2012, **23**, 1290–1299.
26 S. H. Kim, M. Ou, D. A. Bull and S. W. Kim, *Macromol. Biosci.*, 2010, **10**, 898–905.
27 J. Zhang, L. Wu, F. Meng, Z. Wang, C. Deng, H. Liu and Z. Zhong, *Langmuir*, 2012, **28**, 2056–2065.
28 J. Chen, F. Zehtabi, J. Ouyang, J. M. Kong, W. Zhong and M. M. Q. Xing, *J. Mater. Chem.*, 2012, **22**, 7121–7129.
29 J. Li, M. R. Huo, J. Wang, J. P. Zhou, J. M. Mohammad, Y. L. Zhang, Q. N. Zhu, A. Y. Waddad and Q. Zhang, *Biomaterials*, 2012, **33**, 2310–2320.
30 J. H. Ryu, S. Bickerton, J. M. Zhuang and S. Thayumanavan, *Biomacromolecules*, 2012, **13**, 1515–1522.
31 L. Gao, J. B. Fei, J. Zhao, W. Cui, Y. Cui and J. B. Li, *Chem.–Eur. J.*, 2012, **18**, 3185–3192.
32 F. Shi, J. Ding, C. Xiao, X. Zhuang, C. He, L. Chen and X. Chen, *J. Mater. Chem.*, 2012, **22**, 14168–14179.
33 M. Ding, J. Li, X. Fu, J. Zhou, H. Tan, Q. Gu and Q. Fu, *Biomacromolecules*, 2009, **10**, 2857–2865.
34 K. K. Sandhu, C. M. McIntosh, J. M. Simard, S. W. Smith and V. M. Rotello, *Bioconjugate Chem.*, 2002, **13**, 3–6.
35 K. Dayananda, M. S. Kim, B. S. Kim and D. S. Lee, *Macromol. Res.*, 2007, **15**, 385–391.
36 S. C. Han, W. D. He, J. Li, L. Y. Li, X. L. Sun, B. Y. Zhang and T. T. Pan, *J. Polym. Sci., Part A: Polym. Chem.*, 2009, **47**, 4074–4082.
37 H. Wei, R. Ravarian, S. Dehn, S. Perrier and F. Dehghani, *J. Polym. Sci., Part A: Polym. Chem.*, 2011, **49**, 1809–1820.
38 T. Xing, B. Lai, X. D. Ye and L. F. Yan, *Macromol. Biosci.*, 2011, **11**, 962–969.
39 V. Butun, S. P. Armes and N. C. Billingham, *Polymer*, 2001, **42**, 5993–6008.
40 S. Y. Liu, J. V. M. Weaver, Y. Q. Tang, N. C. Billingham, S. P. Armes and K. Tribe, *Macromolecules*, 2002, **35**, 6121–6131.
41 C. H. Li, Z. S. Ge, J. Fang and S. Y. Liu, *Macromolecules*, 2009, **42**, 2916–2924.
42 M. Xiong, Y. Bao, X. Yang, Y. Wang, B. Sun and J. Wang, *J. Am. Chem. Soc.*, 2012, **134**, 4355–4362.
43 L. Zha, B. Banik and F. Alexis, *Soft Matter*, 2011, **7**, 5908–5916.
44 M. H. Smith and L. A. Lyon, *Acc. Chem. Res.*, 2012, **45**, 985–993.
45 Y. Pang, J. Liu, Y. Su, J. Wu, L. Zhu, X. Zhu, D. Yan and B. Zhu, *Polym. Chem.*, 2011, **2**, 1661–1670.
46 L. Chang, L. Deng, W. Wang, Z. Lv, F. Hu, A. Dong and J. Zhang, *Biomacromolecules*, 2012, **13**, 3301–3310.
47 L. J. Zhu, C. L. Tu, B. S. Zhu, Y. Su, Y. Pang, D. Y. Yan, J. L. Wu and X. Y. Zhu, *Polym. Chem.*, 2011, **2**, 1761–1768.
48 L. M. Pan, Q. J. He, J. N. Liu, Y. Chen, M. Ma, L. L. Zhang and J. L. Shi, *J. Am. Chem. Soc.*, 2012, **134**, 5722–5725.
49 A. J. Kirby, P. Camilleri, J. B. F. N. Engberts, M. C. Feiters, R. J. M. Nolte, O. Söderman, M. Bergsma, P. C. Bell, M. L. Fielden, C. L. García Rodríguez, P. Guédat, A. Kremer, C. McGregor, C. Perrin, G. Ronsin and M. C. P. van Eijk, *Angew. Chem., Int. Ed.*, 2003, **42**, 1448–1457.
50 H. Zheng and S. Che, *RSC Adv.*, 2012, **2**, 4421.
51 R. P. Johnson, Y. I. Jeong, E. Choi, C. W. Chung, D. H. Kang, S. O. Oh, H. Suh and I. Kim, *Adv. Funct. Mater.*, 2012, **22**, 1058–1068.